Oberwolfach Preprints

OWP 2007 - 11

ELVIRA BARBERA AND INGO MÜLLER

Secondary Heat Flow Between Confocal Ellipses - an Application of Extended Thermodynamics

Mathematisches Forschungsinstitut Oberwolfach gGmbH
Oberwolfach Preprints (OWP) ISSN 1864-7596

Oberwolfach Preprints (OWP)

Starting in 2007, the MFO publishes a preprint series which mainly contains research results related to a longer stay in Oberwolfach. In particular, this concerns the Research in Pairs-Programme (RiP) and the Oberwolfach-Leibniz-Fellows (OWLF), but this can also include an Oberwolfach Lecture, for example.

A preprint can have a size from 1 - 200 pages, and the MFO will publish it on its website as well as by hard copy. Every RiP group or Oberwolfach-Leibniz-Fellow may receive on request 30 free hard copies (DIN A4, black and white copy) by surface mail.

Of course, the full copy right is left to the authors. The MFO only needs the right to publish it on its website *www.mfo.de* as a documentation of the research work done at the MFO, which you are accepting by sending us your file.

In case of interest, please send a **pdf file** of your preprint by email to *rip@mfo.de* or *owlf@mfo.de*, respectively. The file should be sent to the MFO within 12 months after your stay as RiP or OWLF at the MFO.

There are no requirements for the format of the preprint, except that the introduction should contain a short appreciation and that the paper size (respectively format) should be DIN A4, "letter" or "article".

On the front page of the hard copies, which contains the logo of the MFO, title and authors, we shall add a running number (20XX - XX).

We cordially invite the researchers within the RiP or OWLF programme to make use of this offer and would like to thank you in advance for your cooperation.

Imprint:

Mathematisches Forschungsinstitut Oberwolfach gGmbH (MFO)
Schwarzwaldstrasse 9-11
77709 Oberwolfach-Walke
Germany

Tel +49 7834 979 50
Fax +49 7834 979 55
Email admin@mfo.de
URL www.mfo.de

The Oberwolfach Preprints (OWP, ISSN 1864-7596) are published by the MFO.

Secondary heat flow between confocal ellipses – an application of extended thermodynamics

Elvira Barbera*, Ingo Müller†

Abstract

Much as non-Newtonian fluids exhibit secondary flows in elliptic pipes, rarefied gases exhibit secondary heat flows between elliptical cylinders. The phenomenon may be called non-Fourierian, because it is not covered by Fourier's law of heat conduction. The effect is demonstrated in the paper by exploiting the 13-moment theory of gases. Apart from secondary heat flows the theory predicts shear stresses balanced by gradients of the heat flux, and the need for a distinction of the kinetic and the thermodynamic temperature.

1 Introduction

1.1 The problem

The kinetic theory of gases and extended thermodynamics predict symmetric hyperbolic equations for the mathematical description of the behaviour of a gas. And the 13-moment theory of Grad [1] provides the simplest such set of equations; it is appropriate for moderately rarefied gases. Mathematicians and engineers like to "regularize" these equations, i.e. make them parabolic. In this manner the 13-moment theory becomes the classical theory of Navier-Stokes-Fourier, whose best-known deficiency is the infinite speed of heat propagation and of shear waves. This problem has been satisfactorily resolved, cf. [2] and the solution has provided increased confidence in the equations of extended thermodynamics and, in particular, in those of the 13-moment theory.

Even for stationary processes – i.e. excluding waves – there are differences between Navier-Stokes-Fourier and 13 moments. They occur when steep gradients of temperature appear. This means that 13 moments must be employed in rarefied gases when a significant change of temperature occurs over a mean free path of the atoms.

Qualitative phenomena that distinguish 13 moments from Navier-Stokes-Fourier include:

*Dipartimento di Scienze per l'Ingegneria e per l'Architettura, Università di Messina, c/da Di Dio, S. Agata, 98166 Messina, Italy. E-mail: ebarbera@unime.it.

†Technical University of Berlin, 10623 Berlin, Germany. E-mail: Ingo.Mueller@alumni.tu-berlin.de.

- shear stresses and normal components of the deviatoric stress in a gas at rest,
- heat fluxes not described by the Fourier law, so that secondary flows of heat occur,
- the need to distinguish between the kinetic temperature − a measure for the mean speed of the atoms − and thermodynamic temperature, which is continuous at a thermodynamic wall.

These phenomena will be discussed in the paper.

The easiest manner to create steep gradients of temperature in a gas is by letting the boundary or parts of the boundary be strongly curved. The simplest case occurs for heat conduction between co-axial circular cylinders of which the inner one is fairly small. That case will be reviewed in the next subsection; it has been treated in an earlier paper [3].

In the present paper we consider heat conduction between confocal elliptical cylinders. Here the curvature near the short axes is small while it is large near the long axes. This may be seen upon inspection of Fig.1 which otherwise serves to introduce notation and remind the reader of the coordinate net formed by ellipses and hyperbolae.

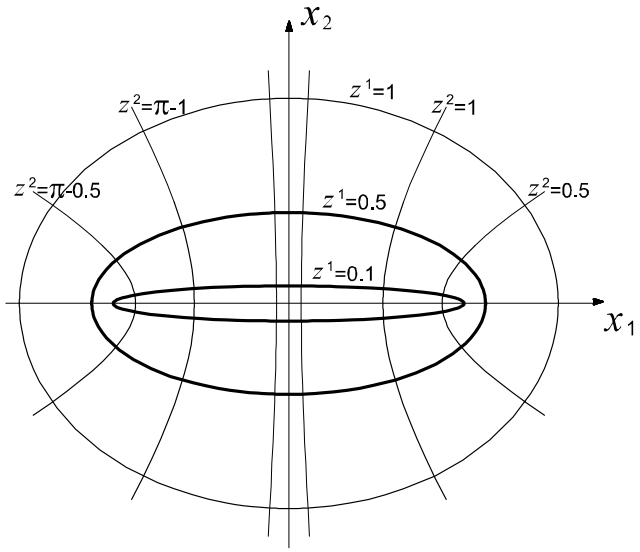

Figure 1: Elliptic hyperbolic coordinates. The fat ellipses $z^1 = 0.1$ and $z^1 = 0.5$ enclose the elliptical ring considered in this paper.

1.2 Stationary heat conduction and thermodynamic temperature between co-axial circular cylinders

The most simple case, where small and large gradients of temperature occur in the same problem, is the case of radial heat conduction in a gas at rest between co-axial circular

cylinders. In that case – which was studied in [3] – the well-known Fourier solution of the energy balance predicts the universal solution[1]

$$\theta = \theta_i + (\theta_e - \theta_i)\,\frac{\ln \frac{r}{r_i}}{\ln \frac{r_e}{r_i}}. \tag{1.1}$$

The 13-moment theory predicts a temperature field of the form

$$\theta = \theta_i - \tfrac{c}{5\tau p} \ln \tfrac{\frac{28}{25}\frac{\tau}{p}c + r^2}{\frac{28}{25}\frac{\tau}{p}c + r_i^2} \quad \text{with } c \text{ from} \quad \theta_e = \theta_i - \tfrac{c}{5\tau p} \ln \tfrac{\frac{28}{25}\frac{\tau}{p}c + r_e^2}{\frac{28}{25}\frac{\tau}{p}c + r_i^2}, \tag{1.2}$$

where τ is the mean time of free flight of the atoms. p is the pressure.

Figure 2 shows the solutions (1.1) and (1.2) graphically for $\tau = 10^{-5}$s and $p = 1$hPa, and it illustrates that both cases differ considerably in the range where the gradient is steep.

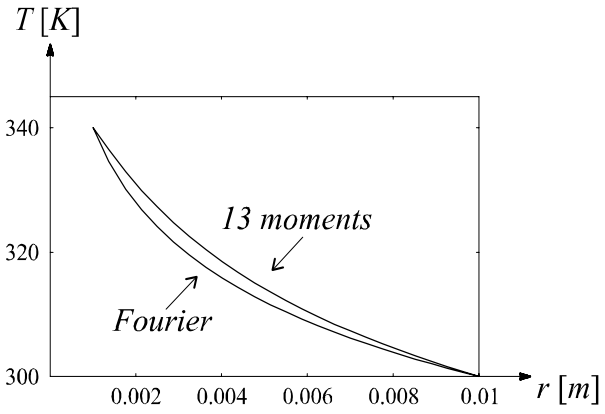

Figure 2: Temperature T between two circular cylinders $r_i = 10^{-3}$m, $r_e = 10^{-2}$m, $p = 1$hPa, $\tau = 10^{-5}$s and $T_i = 340$K, $T_e = 300$K.

Apart from the different temperature fields of the theories of Fourier and 13 moments, it is noteworthy that the 13-moment theory predicts a difference between the *kinetic* temperature T – a measure for the mean kinetic energy of the atoms – and the *thermodynamic* temperature t. The latter is defined by the relation

$$\phi^k = \frac{1}{t} q^k \tag{1.3}$$

between the entropy flux ϕ^k and the heat flux q^k. Therefore t is continuous at a thermodynamic wall in which no entropy production is expected to occur. Thus t is the temperature measured by a contact thermometer.

[1] i and e refer to the inner and the outer cylinder, respectively. And θ stands for $k/\mu T$, where k is the Boltzmann constant, μ the atomic mass and T the kinetic temperature.

For the entropy flux, the 13-moment theory predicts, cf. [2]

$$\phi^k = \frac{1}{T}\left(q^k - \frac{2}{5}\frac{\rho^{<kl>}}{p}q_l\right), \tag{1.4}$$

where $-\rho^{<kl>}$ is the stress tensor; $\rho^{<kl>}$ vanishes in a gas at rest according to the Navier-Stokes theory but it does not vanish in the 13-moment theory; the components $\rho^{<11>}$ and $\rho^{<22>}$ are unequal to zero. Therefore in non-equilibrium there is a difference between T and t and the difference is not small. Figure 3 shows the ratio $\frac{t}{T}$ for the heat conduction problem represented in Fig.2.

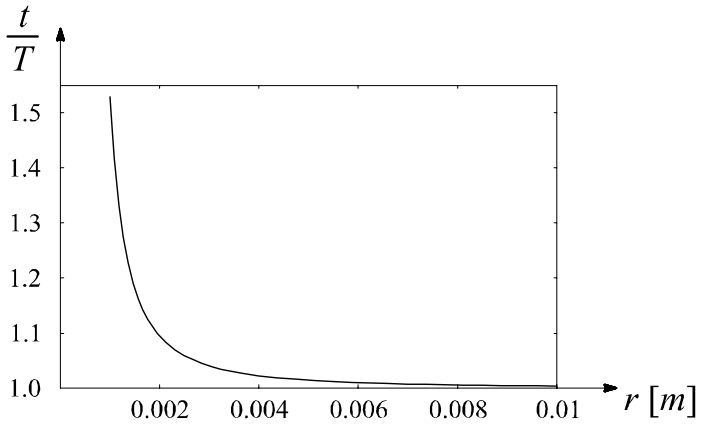

Figure 3: Ratio of thermodynamic and kinetic temperatures.

Furthermore it has been proved in [4] that − in contrast to the Navier-Stokes-Fourier theory − no rigid rotation of the gas between the cylinders is possible according to the 13-moment theory when a radial heat conduction takes place.

These results for circular symmetry have provoked an interest in extended thermodynamics of 13 moments for less symmetric cases. The simplest among those seems to be heat conduction in a gas at rest between confocal ellipses. That case is investigated in the present paper. It turns out that it is characterized by a truely two-dimensional temperature field with shear stresses, and by an even more complex entropy flux than in the circular case; even for the linearized theory.

2 Stationary heat conduction between confocal ellipses

2.1 Field equations

The 13-moment field equations for stationary heat conduction in a gas at rest read in the BGK approximation [5], i.e. with τ=const[2]

$$\begin{array}{lll}
\text{mass balance:} & \text{identically satisfied} & \\
\text{momentum balance:} & g^{ik}\frac{\partial p}{\partial z^k} + \rho^{<ik>}{}_{;k} = 0 & \\
\text{energy balance:} & q^k{}_{;k} = 0 & \\
\text{stress-balance:} & \rho^{<ij>k}{}_{;k} = -\frac{1}{\tau}\rho^{<ij>} & \text{with } \rho^{ijk} = \frac{2}{5}\left(q^i g^{jk} + q^j g^{ki} + q^k g^{ij}\right) \\
\text{heat flux-balance:} & \rho^{ikn}{}_{n;k} = -\frac{2}{\tau}q^k & \text{with } \rho^{ikn}{}_{n} = 5p\theta g^{ik} + 7\theta\rho^{<ik>}.
\end{array} \tag{2.1}$$

For the present planar case of confocal ellipses it is appropriate to employ elliptic-hyperbolic coordinates (z^1, z^2) defined in terms of cartesian coordinates (x^1, x^2) by

$$\begin{array}{l} x^1 = e\cosh z^1 \cos z^2 \\ x^1 = e\sinh z^1 \sin z^2 \end{array} \quad \text{such that} \quad \begin{array}{l} \frac{x_1^2}{\cosh^2 z^1} + \frac{x_2^2}{\sinh^2 z^1} = e^2 \\ \frac{x_1^2}{\cos^2 z^2} - \frac{x_2^2}{\sin^2 z^2} = e^2, \end{array} \tag{2.2}$$

where e is the eccentricity, taken as 10^{-2}m throughout this paper. The corresponding metric tensor is diagonal and the Christoffel symbols are of two types. We have

$$g^{11} = g^{22} = \frac{2}{e^2}\frac{1}{\cosh 2z^1 - \cos 2z^2} \qquad \begin{array}{l} \Gamma^1_{11} = -\Gamma^1_{22} = \Gamma^2_{12} = \Gamma^2_{21} = \frac{\sinh 2z^1}{\cosh 2z^1 - \cos 2z^2}, \\ \Gamma^2_{22} = -\Gamma^2_{11} = \Gamma^1_{12} = \Gamma^1_{21} = \frac{\sin 2z^2}{\cosh 2z^1 - \cos 2z^2}. \end{array} \tag{2.3}$$

We shall abbreviate g^{11} by g.

[2] As usual in curvilinear coordinates we distinguish contra- and co-variant components by upper and lower indices. The semi-colon represents covariant derivatives, and the angular brackets, e.g. in $\rho^{<ij>}$, denote tracefree symmetric tensors.

In explicit form the field equations thus read

$$
\begin{aligned}
&g\tfrac{\partial p}{\partial z^1}+\tfrac{\partial \rho^{<11>}}{\partial z^1}+\tfrac{\partial \rho^{<12>}}{\partial z^2}+4\Gamma^1_{11}\rho^{<11>}+4\Gamma^2_{22}\rho^{<12>}=0,\\
&g\tfrac{\partial p}{\partial z^2}+\tfrac{\partial \rho^{<12>}}{\partial z^1}-\tfrac{\partial \rho^{<11>}}{\partial z^2}+4\Gamma^1_{11}\rho^{<12>}-4\Gamma^2_{22}\rho^{<11>}=0,\\
&\tfrac{\partial}{\partial z^1}\left(\tfrac{q^1}{g}\right)+\tfrac{\partial}{\partial z^2}\left(\tfrac{q^2}{g}\right)=0,\\
&\tfrac{2}{5}g\left(\tfrac{\partial q^1}{\partial z^1}-\tfrac{\partial q^2}{\partial z^2}\right)=-\tfrac{1}{\tau}\rho^{<11>},\\
&\tfrac{2}{5}g\left(\tfrac{\partial q^2}{\partial z^1}+\tfrac{\partial q^1}{\partial z^2}\right)=-\tfrac{1}{\tau}\rho^{<12>},\\
&5gp\tfrac{\partial\theta}{\partial z^1}-2g\theta\tfrac{\partial p}{\partial z^1}\underline{+7\rho^{<11>}\tfrac{\partial\theta}{\partial z^1}+7\rho^{<12>}\tfrac{\partial\theta}{\partial z^2}}=-\tfrac{2}{\tau}q^1,\\
&5gp\tfrac{\partial\theta}{\partial z^2}-2g\theta\tfrac{\partial p}{\partial z^2}\underline{+7\rho^{<12>}\tfrac{\partial\theta}{\partial z^1}-7\rho^{<11>}\tfrac{\partial\theta}{\partial z^2}}=-\tfrac{2}{\tau}q^2.
\end{aligned}
\tag{2.4}
$$

It turns out that $\rho^{<22>}=-\rho^{<11>}$ holds, and that relation has already been used in (2.4) so that $\rho^{<22>}$ does not occur. This means that a planar solution is possible.

2.2 Linearized field equations

For linearization about equilibrium we drop the underlined terms in $(2.4)_{6,7}$ because they are products of quantities that vanish in equilibrium. Also the coefficients p and θ in those equations must be taken as constant equilibrium values $p_{\rm E}$ and $\theta_{\rm E}$ in a linear theory. If the thus simplified expressions for q^1 and q^2 are introduced into $(2.4)_{4,5}$ we obtain

$$
\begin{aligned}
\rho^{<11>}&=\tfrac{2}{5}\tau^2g^2\left[-\Gamma^1_{11}\tfrac{\partial K}{\partial z^1}+\tfrac{\partial^2 K}{(\partial z^1)^2}+\Gamma^2_{22}\tfrac{\partial K}{\partial z^2}\right],\\
\rho^{<12>}&=\tfrac{2}{5}\tau^2g^2\left[-\Gamma^1_{11}\tfrac{\partial K}{\partial z^2}+\tfrac{\partial^2 K}{\partial z^1\partial z^2}-\Gamma^2_{22}\tfrac{\partial K}{\partial z^1}\right],
\end{aligned}
\qquad \text{where} \quad K=5p_{\rm E}\theta-2\theta_{\rm E}p. \tag{2.5}
$$

With these expressions for $\rho^{<11>}$ and $\rho^{<12>}$ a lengthy calculation shows that $(2.4)_{1,2}$ imply that p is constant. Knowing this, we eliminate q^1 and q^2 from the energy balance $(2.4)_3$ and obtain the simple Laplace equation for θ

$$
\frac{\partial^2\theta}{(\partial z^1)^2}+\frac{\partial^2\theta}{(\partial z^2)^2}=0. \tag{2.6}
$$

We envisage a boundary value problem between an outer ellipse $z^1_e=0.5$ at $T_e=300$K and an inner ellipse $z^1_i=0.1$ at $T_i=340$K, and with $\frac{\partial\theta}{\partial z^2}\big|_{z^1,z^2=\pm\frac{\pi}{2}}=0$ on the short half axes. Obviously

$$
\theta=\theta_i+\frac{\theta_e-\theta_i}{z^1_e-z^1_i}\left(z^1-z^1_i\right) \tag{2.7}
$$

is a solution of that problem − and therefore the only solution. Thus the linearized equations are solved.

We proceed to discuss some salient features of the solution.

- The linear dependence of θ on z^1 is also the result of the simple Fourier theory. And we obtain $q^2 = 0$ which is again the same as in the Fourier theory.

- However, in the Navier-Stokes theory, $\rho^{<ij>}$ would obviously be zero, since the gas is at rest. On the other hand, here, in the 13-moment theory we obtain from (2.5)

$$\begin{aligned} \rho^{<11>} &= A p_{\mathrm{E}} g^2 \Gamma^1_{11}, \\ \rho^{<12>} &= A p_{\mathrm{E}} g^2 \Gamma^2_{22}, \end{aligned} \qquad \text{where} \quad A = -2\tau^2 \tfrac{\theta_e - \theta_i}{z^1_e - z^1_i}. \tag{2.8}$$

  So, here we have non-vanishing normal and shear components of the deviatoric pressure tensor; they are balanced, so to speak, by gradients of the heat flux, cf. $(2.4)_{4,5}$.

- As always in the 13-moment theory the entropy flux is given by (1.4)[3]. In the present case this implies

$$\phi^1 = \underbrace{\frac{1}{T}\left(1 - \frac{2}{5}\frac{\rho^{<11>}}{p_{\mathrm{E}}}\frac{1}{g}\right)}_{\dfrac{1}{t}} q^1. \tag{2.9}$$

  Therefore t, defined as indicated in (2.9), is the thermodynamic temperature and we obtain for the ratio of the thermodynamic and the kinetic temperatures

$$\frac{t}{T} = \frac{1}{1 + \frac{4}{5}\tau^2 \frac{\theta_e - \theta_i}{z^1_e - z^1_i} g \Gamma^1_{11}}. \tag{2.10}$$

In Fig.4 we show plots of the shear component $\rho^{<12>}(z^1, z^2)$ of the pressure tensor and of the ratio $\frac{t}{T}$. Inspection shows that the "non-Fourierian features" of the solution occur mostly on the long half axis of the ellipses near the inner ellipse whose curvature is large there. The pressure p_{E} is taken as 1hPa and τ is chosen as $2 \cdot 10^{-6}$s. Figure 4(a) represents the contravariant component $\rho^{<12>}$; therefore the shear stress has the dimensions $\mathrm{N/m^4}$.

In the plot of $\frac{t}{T}$ in Fig.4(b) the cut $z^2 = 0$ – along the long axis – exhibits sharply increasing values of that ratio near the inner ellipse. This is to be expected; the phenomenon is akin – qualitatively – to the circular case shown in Fig.3. It is noteworthy, however, that there is no noticeable increase of $\frac{t}{T}$ on the short axis. All fields are "well-behaved" there, because the small curvature of the inner ellipse at $z^2 = \pm\frac{\pi}{2}$ does not induce significant values of $\rho^{<11>}$ and $\rho^{<12>}$.

The plots of Fig.4 project half of the elliptic ring with $0.1 \leq z^1 \leq 0.5$ and $-\frac{\pi}{2} \leq z^2 \leq \frac{\pi}{2}$ into a rectangle. This offers a good view on the effects of 13-moment theory which are crowded around the sharp tip of the inner ellipse.

[3]Note that even in a linearized theory the entropy inequality, hence the entropy flux, must contain non-linear – second order – terms lest it lose all meaning.

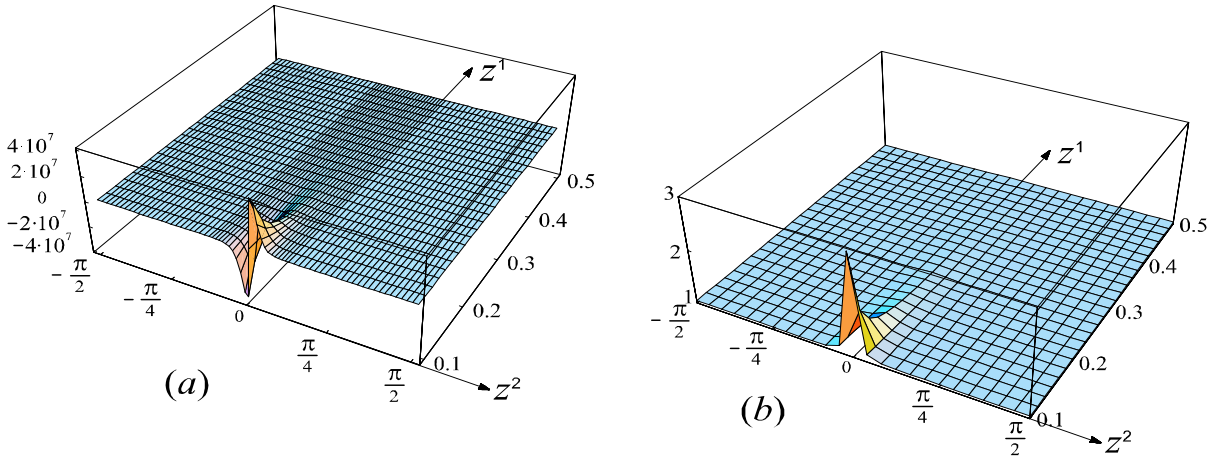

Figure 4: (a) The contravariant shear component $\rho^{<12>}$ of the pressure tensor in N/m^4. (b) The ratio t/T of thermodynamic and kinetic temperature.

The figures show that even the linearized version of the 13-moment theory contains some surprising features that go beyond the prediction of the Navier-Stokes-Fourier theory.

The temperature field, however, in its linear dependence on z^1 is of the classical Fourier type. This will change when we now proceed to investigate the effect of the non-linear terms of the 13-moment equations.

2.3 The effect of non-linear terms

We have not been able to solve the fully non-linear 13-moment theory which is characterized by the set of equations (2.4). So, in order to obtain some indication on non-linear effects we introduce the linear solution (2.8) for $\rho^{<11>}$ and $\rho^{<12>}$ into $(2.4)_{6,7}$ and retain p=const which is consistent − for those values of $\rho^{<11>}$ and $\rho^{<12>}$ − with $(2.4)_{1,2}$. In this manner we uncouple the equations $(2.4)_{3,6,7}$ from the rest of (2.4) and obtain the simple system

$$\begin{aligned}
&\tfrac{\partial}{\partial z^1}\left(\tfrac{q^1}{g}\right)+\tfrac{\partial}{\partial z^2}\left(\tfrac{q^2}{g}\right)=0,\\
&\tfrac{q^1}{g}=-\tfrac{\tau}{2}p_{\mathrm{E}}\left[\left(5+7Ag\Gamma^1_{11}\right)\tfrac{\partial\theta}{\partial z^1}+7Ag\Gamma^2_{22}\tfrac{\partial\theta}{\partial z^2}\right],\\
&\tfrac{q^2}{g}=-\tfrac{\tau}{2}p_{\mathrm{E}}\left[\left(5-7Ag\Gamma^1_{11}\right)\tfrac{\partial\theta}{\partial z^2}+7Ag\Gamma^2_{22}\tfrac{\partial\theta}{\partial z^1}\right].
\end{aligned}\tag{2.11}$$

Accordingly the Laplace equation (2.6) is now replaced by

$$\begin{aligned}
\left(1+\tfrac{7}{5}Ag\Gamma^1_{11}\right)\tfrac{\partial^2\theta}{(\partial z^1)^2}+\tfrac{14}{5}Ag\Gamma^2_{22}\tfrac{\partial^2\theta}{\partial z^1\partial z^2}+\left(1-\tfrac{7}{5}Ag\Gamma^1_{11}\right)\tfrac{\partial^2\theta}{(\partial z^2)^2}+\\
-\tfrac{14}{5}Ag\left[\left(\Gamma^1_{11}\right)^2+\left(\Gamma^2_{22}\right)^2\right]\tfrac{\partial\theta}{\partial z^1}=0.
\end{aligned}\tag{2.12}$$

We solve this equation for the boundary value problem

$$\theta\left(0.5, z^2\right) = \frac{k}{\mu}300\text{K}, \quad \frac{\partial\theta}{\partial z^1}\Big|_{0.5,z^2} = F\left(z^2\right), \quad \frac{\partial\theta}{\partial z^2}\Big|_{z^1,\pm\frac{\pi}{2}} = 0, \tag{2.13}$$

and adjust $F\left(z^2\right)$ in a laborious process of repeated shooting and reaiming so as to reach $\theta\left(0.1, z^2\right) = \frac{k}{\mu}340\text{K}$ on the inner ellipse − at least approximately: to within 0.03K. The solution is numerically obtained with Mathematica® and it is presented in Fig.5. Figure 5(a) shows the "temperature bump" superposed on the linear solution. In Fig.5(b) we see the bump itself from the front and in a different scale so that its size of a few K can be appreciated.

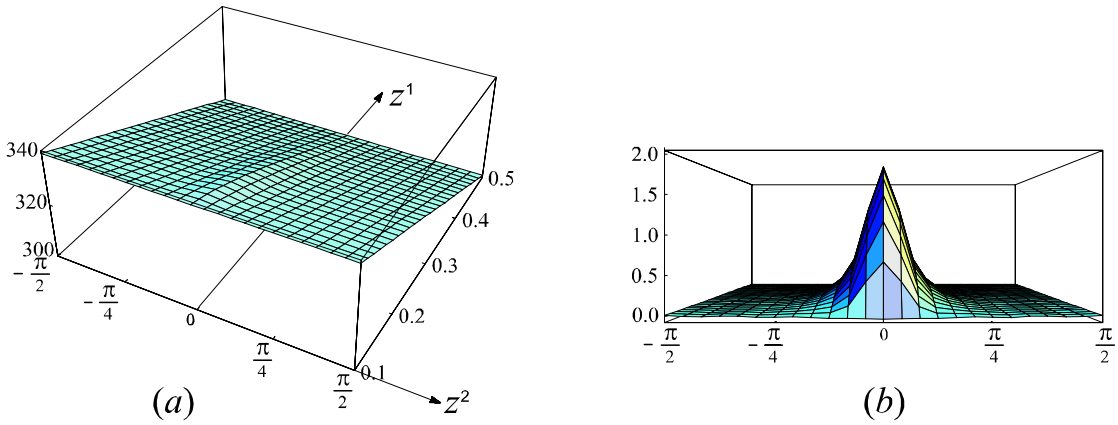

Figure 5: Temperature field in K between elliptical cylinders at $z^1 = 0.1$ and $z^2 = 0.5$. The "bump" occurs along the long axis at $z^2 = 0$.

We conclude that the temperature field is no longer a function of z^1 alone, it also depends on z^2. That dependence on z^2 is highlighted by drawing $\theta\left(z^1, 0\right)$ on the long axis and $\theta\left(z^1, \frac{\pi}{2}\right)$ on the short axis, cf. Fig.6. The straight lines in the figure represent the Fourier solution. On the short axis that solution cannot be distinguished from the 13-moment solution, while on the long axis there is an appreciable difference. The behaviour on the long axis corresponds to that for circular cylinders, shown in Fig.2, except for a distortion that is due to the different geometry.

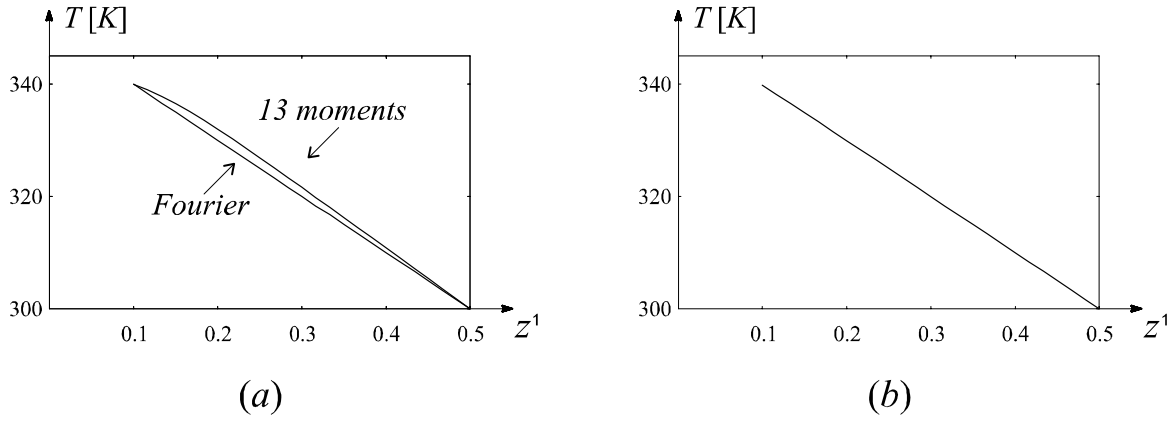

Figure 6: (a) Temperature $\theta\left(z^1, 0\right)$ on the long axis, and (b) $\theta\left(z^1, \pm\frac{\pi}{2}\right)$ on the short axis.

2.4 Primary and secondary heat flux

Since the temperature field $\theta\left(z^1, z^2\right)$ is now known, albeit only numerically, we may calculate the components of its gradient and hence, by $(2.11)_{2,3}$, the components of the heat flux; both are non-zero. The primary contribution to the heat flux has only a 1-component which is the solution of the linearized theory − and of the Fourier theory. It reads

$$q^1\big|_{\text{primary}} = -\frac{5}{2}\tau p_{\text{E}} g \frac{\theta_e - \theta_i}{z_e^1 - z_i^1}. \tag{2.14}$$

Figure 7 shows a vector field plot of $\left(q^1 - q^1\big|_{\text{primary}}, q^2\right)$; it represents the secondary heat flow which is predicted by the 13-moment theory.

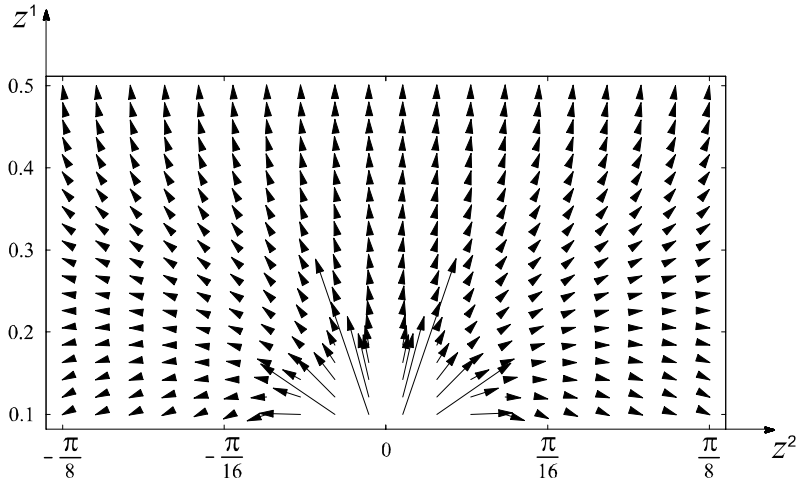

Figure 7: Vector field plot of secondary heat flow.

The most obvious feature of Fig.7 is the non-vanishing 2-component of the heat flux. It has maximal values near the tip of the inner ellipse but it is nowhere zero in the plotted range, except on the axis $z^2 = 0$, of course. Thus there is a genuinely two-dimensional secondary flow of heat.

2.5 Kinetic and thermodynamic temperatures

The above non-linear results, by which $q^2 \neq 0$ holds, add another term to the entropy flux and therefore to the thermodynamic temperature. We now have

$$\phi^1 = \underbrace{\frac{1}{T}\left(1 - \frac{2}{5}\frac{\rho^{<11>}}{p_{\mathrm{E}}}\frac{1}{g} - \frac{2}{5}\frac{\rho^{<12>}}{p_{\mathrm{E}}}\frac{1}{g}\frac{q^2}{q^1}\right)}_{\frac{1}{t}} q^1. \tag{2.15}$$

Thus the thermodynamic temperature depends not only on the components of the pressure deviator but also on those of the heat flux. Certainly, if the kinetic temperature is constant on the inner ellipse, the thermodynamic one is not, and *vice versa*.

2.6 Remark on approximation

Although g and Γ^1_{11} are not singular in the mathematical sense at $(z^1, z^2) = (0.1, 0)$ − the tip of the inner ellipse −, they have sharp peaks there. Therefore our approximation of the non-linear behaviour becomes precarious in the immediate neighbourhood of that point. More rarefied gases than those considered here, − with $p = 10^2\mathrm{N/m}^2$ and $\tau = 2 \cdot 10^{-6}\mathrm{s}$ − will probably call for a more refined theory, i.e. extended thermodynamics with more than 13 moments. Certainly the Fourier theory is inappropriate in this problem and we believe that the present 13-moment theory, whatever its deficiencies are near the critical tip, offers an improvement.

Acknowledgement: We are grateful to the Mathematisches Forschungsinstitut Oberwolfach for having included us in the program "Research in Pairs". This has enabled us to continue our joint research into the properties of Extended Thermodynamics.

References

[1] Grad H. "On the kinetic theory of rarefied gases". *Comm. Pure and Applied Mathematics*, **2**, (1949).

[2] Müller I. Ruggeri T. *Rational Extended Rational Thermodynamics*, Springer, New York, 1998.

[3] Müller I. Ruggeri T. Stationary "Heat Conduction in Radially Symmetric Situations - An Application of Extended Thermodynamics". *J. Non Newtonian Fluid Mech.* **119**, 139-143 (2004).

[4] Barbera E. Müller I., "Inherent Frame Dependence of Thermodynamic Fields in a Gas", *Acta Mechanica*, **184**, 205-216 (2006).

[5] Bhatnagar, P.L. Gross, E.P. and Krook, M., "A model for collision processes in gases. I. Small amplitude processes in charged and neutral one-component systems", *Phys.Rev.*, **94**, (1954).